A&A 392, 215–229 (2002)
DOI: 10.1051/0004-6361:20020876

Astronomy & Astrophysics

The CORALIE survey for southern extra-solar planets⋆

IX. A 1.3-day period brown dwarf disguised as a planet

N. C. Santos[1], M. Mayor[1], D. Naef[1], F. Pepe[1], D. Queloz[1], S. Udry[1], M. Burnet[1], J. V. Clausen[2], B. E. Helt[2], E. H. Olsen[2], and J. D. Pritchard[3]

[1] Observatoire de Genève, 51 Ch. des Maillettes, 1290 Sauverny, Switzerland
[2] Niels Bohr Institute for Astronomy, Physics, and Geophysics; Astronomical Observatory, Juliane Maries Vej 30, 2100 Copenhagen Ø, Denmark
[3] European Southern Observatory, Santiago, Chile

Received 24 April 2002 / Accepted 4 June 2002

Abstract. In this article we present the case of HD 41004 AB, a system composed of a K0V star and a 3.7-mag fainter M-dwarf companion. We have obtained 86 CORALIE spectra of this system with the goal of obtaining precise radial-velocity measurements. Since HD 41004 A and B are separated by only 0.5″, in every spectrum taken for the radial-velocity measurement, we are observing the blended spectra of the two stars. An analysis of the measurements has revealed a velocity variation with an amplitude of about 50 m s^{-1} and a periodicity of 1.3 days. This radial-velocity signal is consistent with the expected variation induced by the presence of a companion to either HD 41004 A or HD 41004 B, or to some other effect due to e.g. activity related phenomena. In particular, such a small velocity amplitude could be the signature of the presence of a very low mass giant planetary companion to HD 41004 A, whose light dominates the spectra. The radial-velocity measurements were then complemented with a photometric campaign and with the analysis of the bisector of the CORALIE Cross-Correlation Function (CCF). While the former revealed no significant variations within the observational precision of ~0.003–0.004 mag (except for an observed flare event), the bisector analysis showed that the line profiles are varying in phase with the radial-velocity. This latter result, complemented with a series of simulations, has shown that we can explain the observations by considering that HD 41004 B has a brown-dwarf companion orbiting with the observed 1.3-day period. As the spectrum of the fainter HD 41004 B "moves" relative to the one of HD 41004 A (with an amplitude of a few km s^{-1}), the relative position of the spectral lines of the two spectra changes, thus changing the blended line-profiles. This variation is large enough to explain the observed radial-velocity and bisector variations, and is compatible with the absence of any photometric signal. If confirmed, this detection represents the first discovery of a brown dwarf in a very short period (1.3-day) orbit around an M dwarf. Finally, this case should be taken as a serious warning about the importance of analyzing the bisector when looking for planets using radial-velocity techniques.

Key words. techniques: radial velocities – binaries: visual – binaries: spectroscopic – stars: brown dwarfs – stars: exoplanets – stars: individual: HD 41004

1. Introduction

Radial-velocity techniques have so far unveiled about 100 planetary companions around solar type dwarfs[1]. The most precise instruments currently available for planet searches can measure the velocity of a star in the direction of the line-of-sight with a precision of the order of 2–3 m s^{-1} (e.g. Queloz et al. 2001a; Butler et al. 2001; Pepe et al. 2002), but even higher precision is expected from instruments available in the near future (e.g. HARPS – Pepe et al. 2000a). This will definitely allow the discovery of lower mass and longer period planets, that remained undetected up to now due to the low amplitude of the induced radial-velocity variation.

The gain in precision will, however, bring to light some of the limitations of the radial-velocity method. It is well known, for example, that radial-velocity "jitter" with amplitudes up to a few tens of m s^{-1} is expected to result from the presence of strong photospheric features like spots or convective inhomogeneities, associated with chromospheric activity phenomena (Saar & Donahue 1997; Saar et al. 1998; Santos et al. 2000). The presence of spots can even induce a periodic radial-velocity signal similar to the one expected from the presence of a planet. This is the case for HD 166435

Send offprint requests to: N. C. Santos,
e-mail: Nuno.Santos@obs.unige.ch

⋆ Based on observations collected at the La Silla Observatory, ESO (Chile), with the CORALIE spectrograph at the 1.2-m Euler Swiss telescope and with the Strömgren Automatic Telescope (SAT).

[1] See e.g. obswww.unige.ch/~udry/planet/planet.html

Table 1. Stellar parameters for HD 41004 A.

Parameter	Value	Reference
Spectral type	K1V/K2V	Hipparcos (ESA 1997)/ *uvby* (see Sect. 2.4)
Parallax [mas]	23.24 ± 1.02	Hipparcos (ESA 1997)
Distance [pc]	43	Hipparcos (ESA 1997)
m_v	8.65	Hipparcos (ESA 1997)
$B-V$	0.887	Hipparcos (ESA 1997)
$T_{\rm eff}$ [K]	5010	See text
$\log g$ [cgs]	4.42	See text
M_v	5.48	–
Luminosity [$L_\odot$]	0.65	Flower (1996)
Mass [$M_\odot$]	~0.7	–
$\log R'_{\rm HK}$	−4.66	Henry et al. (1996)
Age [Gyr]	1.6	Donahue (1993)
$P_{\rm rot}$ [days]	~27	Noyes et al. (1984)
$v \sin i$ [km s^{-1}]	1.22	CORALIE
[Fe/H]	−0.09/+0.10	*uvby*/CORALIE

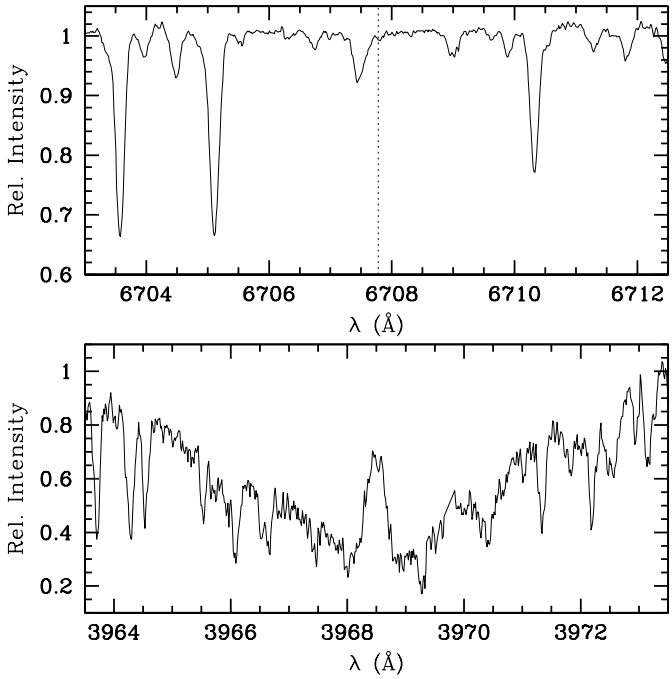

Fig. 1. *Upper panel*: added CORALIE spectrum in the Lithium line region for HD 41004. The plot reveals no clear Li detection for this star. *Lower panel*: added CORALIE spectrum in the Ca II H line central region for HD 41004. The strong emission near line center suggests that the star is chromospherically active.

(Queloz et al. 2001b), a star presenting a radial-velocity signal with a period of about 3.8-days, but showing both photometric and bisector variations with the same periodicity.

The case of HD 166435 illustrates very well the need to confirm, at least for the shortest period cases, that the radial-velocity signature is indeed due to the presence of a low mass companion, and not due to some kind of intrinsic phenomena. As shown by Queloz et al. (2001b), the use of photometric data and bisector analysis was crucial to clarify the origin of the radial-velocity variations observed on this star.

In this paper we present the case of HD 41004, a visual double system consisting of a K1V-M2V pair (A and B components). This system was found to present a radial-velocity signature similar to the one expected as if the K1 dwarf had a very low mass planetary companion in a 1.3-day period orbit. Although the photometric data revealed no significant photometric variations, an analysis of the Bisector Inverse Slope (BIS) of the CORALIE Cross-Correlation Function (CCF) (Queloz et al. 2001b) revealed a periodic variation in phase with the radial-velocity signal. In the following sections we will show that the radial-velocity variation is in fact not a result of the periodic motion of the A component, but of the Doppler motion of the spectrum of the B component due to the presence of a brown-dwarf companion. The results strongly caution about the need to use methods capable of detecting line asymmetries, like the bisector analysis, when dealing with high-precision planet searches with radial-velocity techniques.

2. The case of HD 41004

2.1. Stellar characteristics

In the Hipparcos catalogue HD 41004 (HIP 28393, CD −48 2083) is presented as the A component of a double system, where the 3.68 mag fainter companion is at a separation of about 0.5″. From the magnitude difference, and considering that both stars are at the same distance (i.e. that they constitute a physical double system) we can deduce that HD 41004 B is probably a M2 dwarf. In the rest of this paper we will denote by HD 41004 AB the system composed by HD 41004 A and HD 41004 B.

The small angular separation between the two components implies that we cannot separate (with the instrumentation used) the light coming from the two stars. However, given the relatively "large" magnitude difference, we do not expect the flux coming from HD 41004 B (about 3% of that coming from the A component) to affect significantly the determination of the stellar parameters of HD 41004 A. All the parameters described below are thus, in a good approximation, those of HD 41004 A (the star whose light dominates).

At a distance of ~43 parsec – π = 23.24 ± 1.02 mas – ESA (1997), HD 41004 A is a K1 dwarf shining with a visual magnitude V = 8.65 in the southern constellation Pictoris (the Painter's Easel). Its colour index is $B-V$ = 0.887, as listed by the Hipparcos catalogue and its absolute magnitude M_v = 5.48. The basic stellar parameters are summarized in Table 1.

There are not many references in the literature on HD 41004 A, and no precise spectroscopic analysis is available for this star. Using the $b-y$ colour from Olsen (1994b)[2] and the calibration of Alonso et al. (1996) we obtain a temperature of 5030 K, 100 K higher than the 4930 K obtained from the same colour but using the calibration of Olsen (1984). Using the $B-V$ colour we would obtain $T_{\rm eff}$ = 5075 K from the

[2] A similar $b-y$ was obtained by us – see Sect. 2.4.

Table 2. Elements of the fitted orbit.

P	1.3298	± 0.0002	d
$a_1 \sin i$	0.0009	± 0.0000	Gm
T	2452200.43	± 0.13	d
$e^\dagger$	0.07	± 0.04	
V_r	42.532	± 0.002	km s^{-1}
$\omega^\dagger$	23	± 35	degr
K_1	50	± 2	m s^{-1}
$f_1(m)$	0.1741×10^{-10}	$\pm 0.0224 \times 10^{-10}$	$M_\odot$
σ(O–C)	14		m s^{-1}
N	86		

† Consistent with a circular orbit according to the Lucy & Sweeney (1971) test.

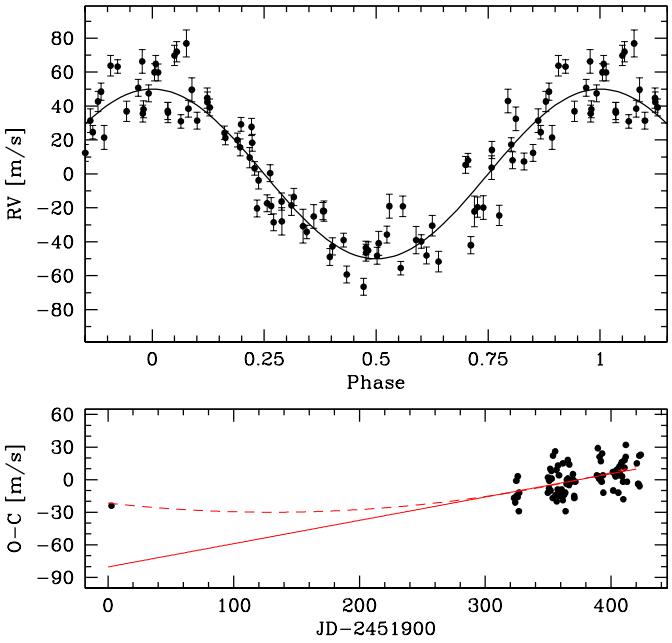

Fig. 2. *Upper panel*: phased CORALIE radial-velocity measurements (subtracted by the γ-velocity) for HD 41004 AB and best Keplerian fit. *Lower panel*: O–C residuals of the CORALIE radial-velocity data over time. The lines represent the best linear fit without considering the first measurement (solid line) and a parabolic fit (dashed line). The linear fit has a slope of 0.2 m s^{-1} day^{-1}.

calibration of Flower (1996). We have decided to use an average value in the following of this paper ($T_{\rm eff}$ = 5010 K). Photometric calibrations can also be used to estimate the surface gravity of a dwarf. Using the calibration of Olsen (1984) we have obtained $\log g = 4.54$, slightly higher than (but compatible with) the value of 4.30 obtained from the Hipparcos parallax (e.g. Allende Prieto et al. 1999) – again, an average value was considered. The obtained $T_{\rm eff}$ and $\log g$ are compatible with a spectral classification of K1V (ESA 1997).

From the photometric calibration of Schuster & Nissen (1989) we have obtained a value of [Fe/H] = −0.09. Another estimation of the metallicity can be obtained from the analysis of the Cross-Correlation Function (CCF) of CORALIE. In fact, its equivalent width (or surface) is very well correlated with the metallicity of the star and its colour $B - V$ (Sect. A.2). Using this method we have derived a higher value of [Fe/H] = +0.10.

Using a metallicity of +0.10, the temperature of 5010 K, and its absolute magnitude, we can estimate a mass of ∼0.7 $M_\odot$ for HD 41004 A using the isochrones of Schaller et al. (1992).

The CCF can also be used to determine the projected rotational velocity $v \sin i$ of a star. From the calibration presented in Sect. A.1, and taking the average Gaussian width of the CCF for our star (4.36 km s^{-1}), we have obtained a value of $v \sin i = 1.22$ km s^{-1}, similar to the 1.54 km s^{-1} obtained from the CORAVEL CCF using the calibration of Benz & Mayor (1984).

An analysis of the Ca II H line core of HD 41004 A reveals a strong emission, suggesting that the star is chromospherically active (see Fig. 1, lower panel). This is confirmed by the value of $\log R'_{\rm HK} = -4.66$ obtained by Henry et al. (1996), and by the fact that a flare event was observed in photometry (see Sect. 2.4). From this value, and using the calibration of Noyes et al. (1984), we can estimate the rotational period to be ∼27 days, a value perfectly compatible with the low $v \sin i$ measured. Using the calibration of Donahue (1993) (also presented in Henry et al. 1996), based on the chromospheric activity level we derive an age of 1.6 Gyr for this star.

In Fig. 1 (upper panel) we show the 6708 Å Li-line region for HD 41004 AB. There is some hint of the presence of Li, but the small feature at the position of the Li line has an equivalent width of less than 2 mÅ. Considering the stellar parameters of our star, this implies an upper limit for the Li abundance of $\log N(\mathrm{Li}) < 0.0$ (this was derived from a LTE spectral analysis using the line abundance code MOOG (Sneden 1973), and a grid of Kurucz (Kurucz 1993) ATLAS9 atmospheres). Given the low temperature of our star, this limit cannot be used as a strong age constraint; the age derived from the activity level is nevertheless compatible with such a low value for the Li abundance (e.g. Jones et al. 1999).

2.2. Radial-velocity data

HD 41004 AB is included in the sample observed in the context of the Geneva extra-solar planet search programme, at La Silla Observatory (Chile), using the CORALIE spectrograph (Udry et al. 2000). From December 2000 to February 2002 we have obtained a total of 86 precise radial-velocity measurements[3] of this system. The average individual photon-noise precision of the radial-velocity measurements is 5.5 m s^{-1}.

Since the angular separation of the two stars is much smaller than the diameter of the CORALIE fiber, in each spectrum obtained we are seeing the blended spectra of HD 41004 A and HD 41004 B. This means that the resulting radial-velocity is not the one of any of the two individual stars, but rather it corresponds to a weighted average of the radial velocities of the two components (although it will be closer to the radial velocity of the A component, since the M dwarf is "only" contributing to ∼3% of the light).

[3] Available in electronic form at the CDS via anonymous ftp to `cdsarc.u-strasbg.fr (130.79.128.5)` or via `http://cdsweb.u-strasbg.fr/cgi-bin/qcat?J/A+A/392/215`

The analysis of the radial-velocity revealed a variation with a period of ∼1.3-days, and an amplitude of 50 m s^{-1} (see Table 2). A fit to the data (Fig. 2 – upper panel) suggested that the radial-velocity variation could be due to the presence of a low mass (0.25 $M_{\rm Jup}$) planetary companion orbiting HD 41004 A at a distance of only about 0.02 AU (i.e. ∼5.5 stellar radius, considering that HD 41004 A has a radii typical for a K1 dwarf – 0.8 $R_{\odot}$) in a circular trajectory. Although this possibility was very tempting, as we will see below the planetary explanation is not the best.

The relatively high O–C residuals of the fit (14 m s^{-1}) are quite difficult to explain in the light of activity phenomena, since we do not expect them to induce such a high radial-velocity "jitter" in a slow rotator K dwarf (Saar et al. 1998; Santos et al. 2000). Actually, part of the noise seems to be coming from the existence of some radial-velocity drift. An analysis of the (O–C) residuals to the fit reveals a clear trend (considering the last group of points only), with a gradient of 75 m s^{-1} yr^{-1} – (Fig. 2 – lower panel). We note that a comparison with old CORAVEL measurements, as well as with the first (isolated) CORALIE measurement, does not corroborate this trend, i.e. the old measurements (see Fig. 2, lower panel) are not aligned with a linear fit to the residuals of the last group of points. This result is compatible with the fact that the radial-velocity signal passed through a minimum. Finally, some noise might also be coming from the influence of the companion to HD 41004 A. As shown by Pepe et al. (2000b), the presence of a close companion might introduce some noise in the computed radial-velocity due to variations of the flux ratio of the two stars within the CORALIE fiber as a function of the seeing conditions. This noise depends on the separation between the two objects, their magnitude difference, and their radial-velocity difference. For this case we do not expect, however, a strong effect, mostly because of the small angular separation between the two objects (the angular separation of the two stars is much smaller than the diameter of the CORALIE fiber, and thus the influence should be always similar and fairly independent e.g. of the seeing conditions).

As mentioned above, HD 41004 B (a M2 dwarf) is located at an angular separation of ∼0.5″. At the distance of HD 41004 AB this corresponds to a projected separation of ∼21 AU, considering that the two stars form a real system[4]. This value corresponds to the minimum "real separation" (since we are not able to know the distance between the two stars in the direction of the line-of-sight) and implies a period of ∼90 yr, using a mass of 0.7 $M_{\odot}$ and 0.4 $M_{\odot}$ for HD 41004 A and B, respectively. Considering a circular orbit, the amplitude of the variation has a value of 2.5 km s^{-1}, and the maximum derivative of the velocity would be 170 m s^{-1} yr^{-1}. This value is perfectly compatible with the observations, suggesting that the radial-velocity trend observed has its origin in the motion of HD 41004 A around its lower mass companion HD 41004 B. But we cannot exclude that (at least part of) the observed trend might have a different origin, like e.g. the presence of a low mass companion to HD 41004 A.

[4] This is corroborated by the simulation presented below, that implies that both stars have similar radial-velocities.

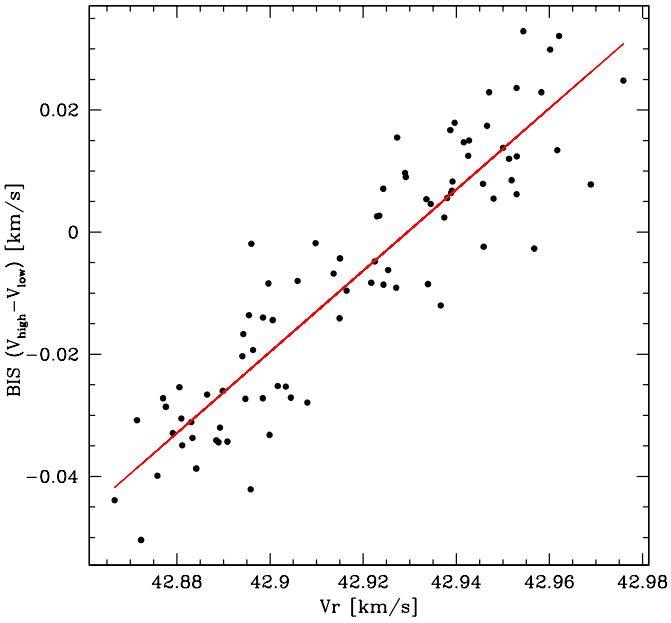

Fig. 3. Measured radial-velocity vs. BIS for HD 41004. The plot shows the two variables vary in phase. The best linear fit is shown. The slope of the line has a value of 0.67.

2.3. Bisector analysis

With such a short period "orbit" (and further knowing that the star is chromospherically active), it was extremely important to analyze the bisector of the CCF for this object. Such an analysis, as presented in Queloz et al. (2001b), is in fact an excellent way of discriminating between radial-velocity variations due to changes in the spectral line shapes from real variations due to the orbital motion of the star. In a few words, we compute the (bisector) velocity for 10 different levels of the Cross-Correlation Function[5]. The values for the upper (near continuum) and lower bisector points are averaged and subtracted (see Fig. 7). The resulting quantity, the Bisector Inverse Slope (BIS), can be used to measure the variations of the line bisector.

The result of the bisector analysis for our star is presented in Fig. 3. As can be seen from the figure, the Bisector Inverse Slope (BIS – Queloz et al. 2001b) – similar to the usual bisector span (Gray 1992) – varies in phase with the radial-velocity. This indicates that most probably the radial-velocity variation observed is being induced by some "intrinsic" phenomena, and not by the presence of a planet around HD 41004 A.

We also note that the radial-velocity in this plot was computed using a different cross-correlation mask than the one used to determine the radial-velocities presented in Fig. 2 (for more details see Queloz et al. 2001b), and the resulting radial-velocity variation amplitude is smaller than the one measured with the standard mask (37 m s^{-1} instead of 50 m s^{-1}). This large difference would not be expected if the radial-velocity signal was induced by the presence of a planet around HD 41004 A, since in that case all the lines would "move" by

[5] We can define 12 levels in total, i.e., dividing the CCF in 11 slices, but for clear reasons we exclude the continuum level and the level corresponding to the tip of the CCF.

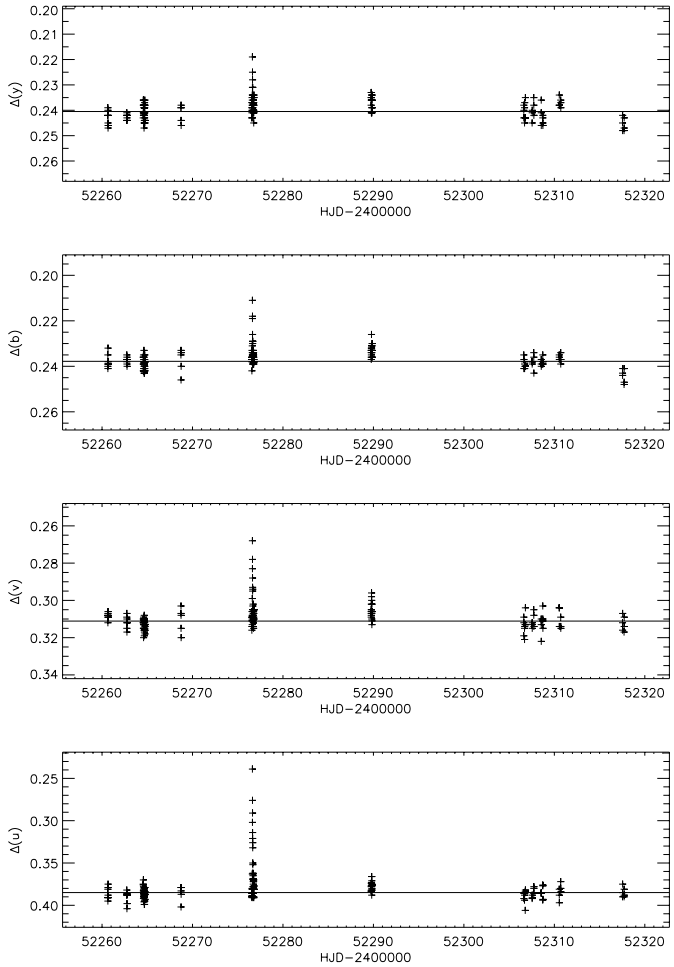

Fig. 4. Magnitude differences HD 41004 AB−HD 39823 in the instrumental system. The horizontal lines represent the mean values (JD 2 452 276 excluded), see text.

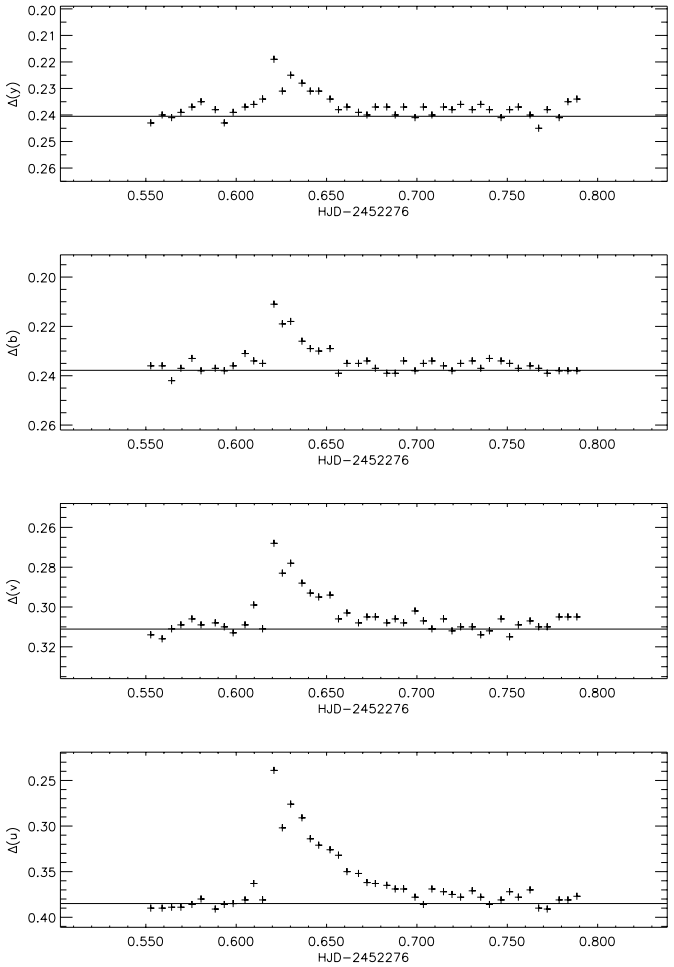

Fig. 5. Magnitude differences HD 41004 AB−HD 39823 in the instrumental system on JD 2 452 276. The horizontal lines represent the mean values (JD 2 452 276 excluded), see text.

the same amount, leaving the radial-velocity variation (but not necessarily the "zero" point) fairly independent of the mask used. The different amplitude observed may be interpreted as a hint that some phenomena is not affecting in the same way all the spectral lines observed.

2.4. Photometry

The observations described above made us suspect that similarly to HD 166435, our star should present photometric variations compatible with the presence of a rotating spot. According to the Hipparcos catalogue (ESA 1997), however, HD 41004 AB is stable, with a magnitude scatter of 0.016 mag, a value that is typical for a star of its magnitude[6]. But this limit is not very telling, since a spot with a filling factor of a few percent can already induce a radial-velocity signal with an amplitude of a few $\mathrm{m\,s^{-1}}$ in our star (Saar & Donahue 1997). Furthermore, we could suppose that this star had just developed a spotted region, that was not present by the time of the Hipparcos measurements.

In order to control the photometric stability[7], we have collected precise photometric data for HD 41004 AB.

The photometric *uvby* observations of HD 41004 AB were obtained at the Strömgren Automatic Telescope (SAT) at ESO, La Silla, Chile on 11 nights between December 2001–February 2002. Details on the spectrometer and the fully-automatic mode of the telescope are given by Olsen (1993, 1994a).

Three comparison stars, HD 39823 (C1), HD 38459 (C2), and HD 43548 (C3) were observed together with HD 41004 AB in the sequence C1–HD 41004–C2–HD 41004–C3–HD 41004–C1, allowing accurate differential magnitude differences to be formed. Each observation consisted of three individual integrations, and the total number of photo-electrons counted per observation was at least 75 000 in *u*, and considerably more in the other three channels. Sky measurements

[6] Again, the photometry is most of all sensitive to the A component of the system, and we are thus basically measuring the eventual photometric variations of HD 41004 A. For example, if the HD 41004 B would change its luminosity by 5%, the total flux of the HD 41004 AB system would change by only ∼0.15%, i.e., about 0.002 magnitudes, a value that is within the observational errors.

[7] These observations were also done with the goal of searching for an eventual planetary transit. Given the short period the probability of transit would be particularly high.

Table 3. Standard *uvby* indices for HD 41004 AB and the comparison stars.

Star	V	$(b-y)$	m_1	c_1	N
HD 41004 AB	8.621	0.524	0.404	0.313	49
	±0.007	±0.004	±0.007	±0.008	
HD 38459	8.493	0.503	0.368	0.329	30
	±0.004	±0.003	±0.006	±0.007	
HD 39823	8.381	0.526	0.315	0.312	38
	±0.004	±0.003	±0.007	±0.006	
HD 43548	8.805	0.434	0.225	0.309	26
	±0.005	±0.004	±0.007	±0.006	

were obtained at a position near HD 41004 AB at least once per sequence. A circular diaphragm of 17″ diameter was used throughout. Nightly linear extinction coefficients were determined from the observations of the comparison stars and other constant stars, and when appropriate, linear or quadratic corrections for drift during the nights were applied.

Differential magnitudes (instrumental system) were formed using for each candidate observation the two nearest comparison star observations. All comparison star observations were used with C2 and C3 first shifted to the level of C1. A careful check of the comparison stars were performed, and during the observing period they were all found to be constant within 0.003–0.004 mag (*vby*) and 0.005–0.006 mag (*u*), which is close to the observational accuracy.

In Fig. 4 we show the 152 obtained HD 41004 AB–HD 39823 magnitude differences in the instrumental system[8]. Typical rms errors of one magnitude difference are 0.004–0.005 (*ybv*) and 0.006–0.008 (*u*). On one night, JD 2 452 276, a sudden brightening of HD 41004 AB was observed, presumably due to a flare. Details are shown in Fig. 5.

Mean magnitude differences HD 41004 AB–HD 39823, excluding the JD 2 452 276 observations, are 0.240 ± 0.004 (*y*), 0.238 ± 0.004 (*b*), 0.311 ± 0.005 (*v*), and 0.385 ± 0.008 (*u*). Thus, the rms errors are close to those expected from the observational uncertainties. We see no sign of variability correlated with the 1.3 day period (Fig. 6). However, as the JD 2 452 276 observations show that HD 41004 AB is active, long term variability at some level can not be excluded.

As an extensive list of *uvby* standard stars were also observed, an accurate transformation to the standard system could be done. The selection of standard stars and the transformation to the standard system will be described in detail elsewhere. Standard *uvby* indices are given in Table 3. For HD 41004 AB they are all within 0.035 mag of the mean *uvby* indices for the MK spectral classification K2V. The colour $(b-y)$ only differs by 0.006 mag from the mean K2V colour index (cf. Olsen 1984).

The results, revealing that the star is stable within the instrumental precision[9], support the idea that the radial-velocity variation observed cannot be due to the presence of spots in the surface of HD 41004 A, as was the case for HD 166435. But it is interesting to mention that indeed we would not expect this to be the case, given that the rotational period of HD 41004 A (see Table 1) is much longer than the observed 1.3-day period in radial-velocity[10]. Otherwise, and given the low $v \sin i$ for this star, we would be observing a system in a very odd configuration. In other words, HD 41004 A is not a HD 166435-analog. This is further supported by the fact that contrarily to HD 166435, the radial-velocity data varies in phase (and not anti-phase) with the BIS (see Fig. 3).

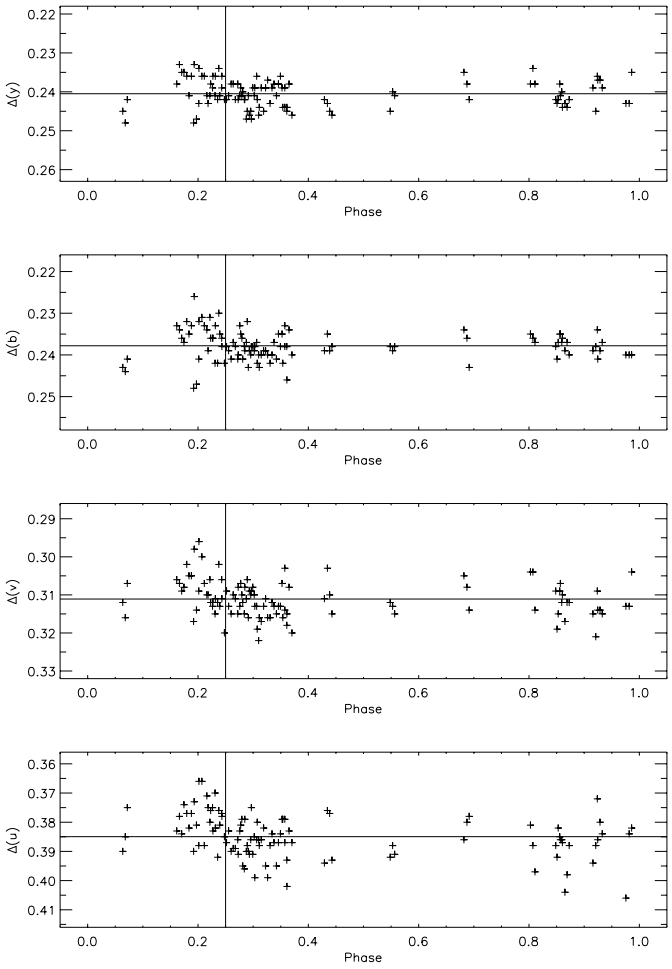

Fig. 6. Phase folded magnitude differences HD 41004 AB−HD 39823 in the instrumental system; JD 2 452 276 observations have been excluded. The horizontal lines represent the mean values, and vertical lines are drawn at phase 0.25, i.e. at the phase of expected central transit.

3. Simulating the observations

The observed correlation between the BIS and the radial-velocity signal, together with the absence of any significant photometric variation lead us to analyze the possibility that

[8] The individual measurements are available in electronic form at CDS via anonymous ftp to
cdsarc.u-strasbg.fr (130.79.128.5) or via
http://cdsweb.u-strasbg.fr/cgi-bin/qcat?J/A+A/392/215

[9] We note also that no transits were found.

[10] We note that the rotational period was obtained from the chromospheric activity level, this latter being derived from an analysis of the Ca II H and K lines. These lines, located in the blue part of the spectrum, are probably not affected at all by the blend with the spectrum of the M dwarf, and will thus give us information only regarding HD 41004 A.

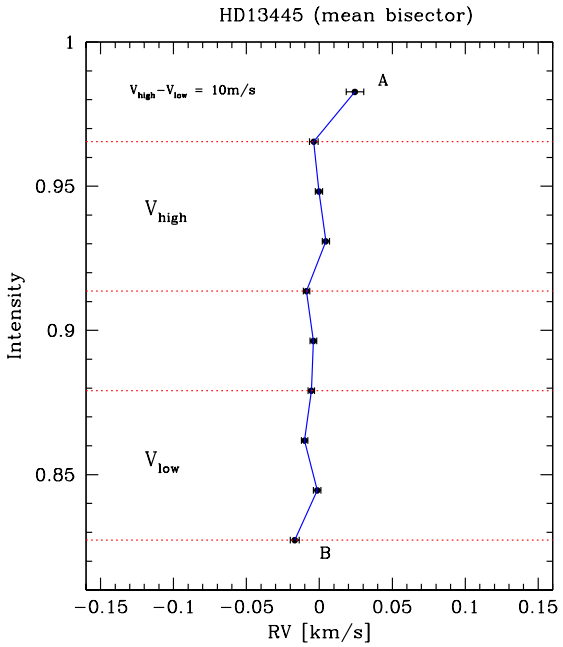

Fig. 7. Average bisector for the K0 dwarf HD 13445. This figure shows that the line bisector is almost vertical for a star of this spectral type. The two regions denoted by the dotted lines ($V_{\rm low}$ and $V_{\rm high}$) represent the intervals used to compute the Bisector Inverse Slope (BIS), defined as BIS = $V_{\rm high}-V_{\rm low}$: $V_{\rm high/low}$ are simply the average of the velocity of the 4 "points" in each of the intervals (for more details see Queloz et al. 2001b). The error bars represent the value of $\sigma(i)/\sqrt{(N)}$, where $\sigma(i)$ is the rms around the mean velocity obtained for a given bisector level i from the N = 118 CCF's available. A and B denote the upper and lower bisector points.

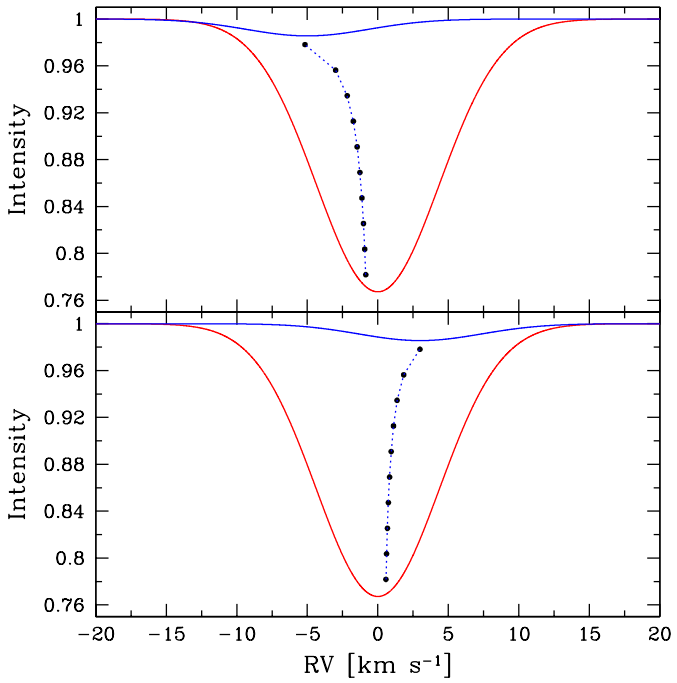

Fig. 8. Figure illustrating the effect of changing the relative position of the CCF's of the HD 41004 A (deeper CCF) and HD 41004 B (smaller CCF): the resulting blended CCF (the addition of the CCF's of the two stars) will change its profile, with the consequent variations in the observed bisector shape (dashed lines). The CCF's and bisectors in this figure are exaggerated for illustration purposes.

the radial-velocity and bisector changes were being induced by a variation in the relative position of the cross-correlation dips of HD 41004 A and HD 41004 B. Since the angular separation between the two objects is only ~0.5″, it is impossible to observe them separately with the 2″ fiber of the CORALIE spectrograph. For each spectrum obtained for HD 41004 AB we have thus the addition of the spectra arriving from the two components. The question was thus to know if a periodic change of the relative position of the two spectra could induce the observed radial-velocity and bisector variations. Two main possibilities can be explored in this sense.

3.1. Case 1

First, we can consider that HD 41004 A has a very low mass companion that is responsible for the observed radial-velocity variation, and that HD 41004 B has a "constant" velocity. If that were the case, what would be the effect on the shape of the bisector (i.e. on the BIS)?

A simple simulation, adding two Gaussian functions (i.e. two cross-correlation dips), the first contributing to only ~3% of the flux[11] (representing HD 41004 B) and the other with ~97% of the flux (representing HD 41004 A), has shown that changing the position of the deeper function by 50 m s^{-1} will reproduce the observed variation in the measured velocity, but leave "constant" the shape of the bisector. This showed us that we can exclude the possibility that the observed radial-velocity variation with a period of 1.3 days is produced by a planetary companion to HD 41004 A.

This simulation suggests that if we hope to simulate the large observed bisector shape variations we need to change the relative position of the two cross-correlation dips by (much) more than 50 m s^{-1}.

3.2. Case 2

To try to verify whether large amplitude periodic variation in the relative position of the two CCFs can induce the observed signal, we have done a set of simulations where two cross-correlation functions were added. As above, these two functions, one corresponding to HD 41004 A and the other to HD 41004 B, were weighted by the relative flux of the two stars (A 30 times brighter than B). These CCF's were considered to be Gaussian for a question of simplicity[12]. This is a good approximation, since the bisector of a K dwarf is observed to be quite vertical (Fig. 7) – see also Gray (1992). However, and as we will see below, this also poses some problems when trying to constrain the results.

In each simulation, the radial-velocity of the primary dip (corresponding to HD 41004 A) was considered to be fixed, and

[11] This value is based, for simplicity, on the magnitude difference between the two objects.

[12] In any case, the real shape of the bisector of HD 41004 A is not known.

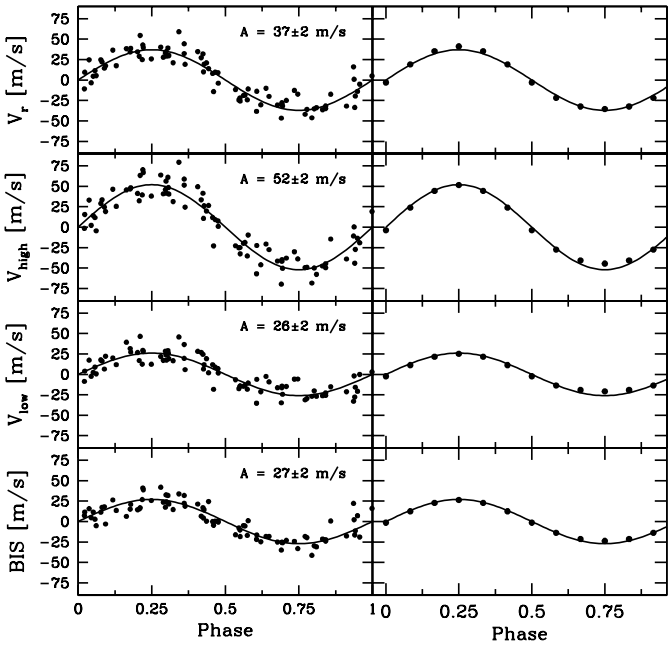

Fig. 9. Comparison between the observed and predicted amplitudes and variations in the radial-velocity, $V_{\rm high}$, $V_{\rm low}$, and BIS. The best fits to the observed data are shown (left), as well as the amplitude of the variations (A); the fitted curves were superposed to the simulated points for comparison. For this simulation, the parameters of the secondary CCF were $\gamma_2 = -2.1\,{\rm km\,s^{-1}}$, $A_2 = 0.14$, $\sigma_2 = 8.0\,{\rm km\,s^{-1}}$ and $K_2 = 4.0\,{\rm km\,s^{-1}}$. The results show the fits to be very good.

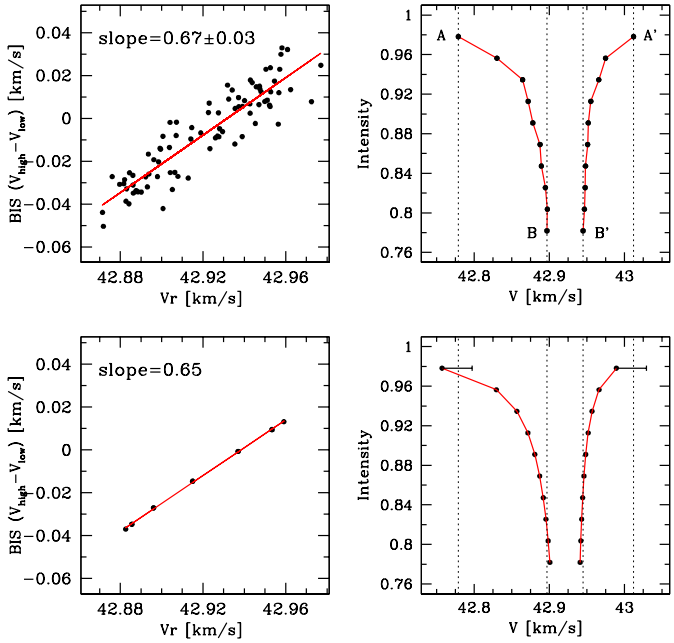

Fig. 10. *Left:* comparison between the observed and simulated slope of the relation between radial-velocity and BIS. *Right:* comparison between the shape of the bisector of the CCF for the maximum and minimum velocities. For the observed case, an average of the bisectors for the measurements corresponding to the maximum/minimum of the velocity was considered. The vertical lines are drawn just to facilitate a comparison. The error-bars drawn represent the uncertainties in the observed bisector, as well as the errors due to the fact that the real "zero" bisector is not vertical as considered in the simulations, but slightly "C" shaped (see text for more details). The parameters of the secondary CCF are the same as in Fig. 9. The velocity scale in these plots is similar to the one of Fig. 7.

the smaller secondary dip, corresponding to HD 41004 B, was taken to vary periodically with a given velocity amplitude (K_2) (see Fig. 8). This variation is supposed to simulate the presence of a companion around HD 41004 B.

A grid of simulations was done by changing both the velocity amplitude K_2 (in the range 2–10 km s^{-1}) and the parameters of the "small" dip (the width σ_2, and the depth A_2 were changed in the range 5–10 km s^{-1} and 0.04–0.20, respectively), as well as the difference between the velocity of the primary CCF and the γ-velocity of the secondary CCF (γ_2, varied between -0.5 and $-3.0\,{\rm km\,s^{-1}}$). In all simulations, the width and depth of the primary dip (σ_1 and A_1) were fixed at $4.36\,{\rm km\,s^{-1}}$ and 0.24, corresponding to the average parameters of the observed CCF of this star (typical parameters for a solar metallicity early K dwarf with low $v \sin i$ – see Appendix).

3.3. Qualitative results

A good example of a successful simulation can be seen in Figs. 9 and 10. In the former we compare the observed (left) and simulated (right) radial-velocities, $V_{\rm high}$, $V_{\rm low}$, and BIS for a simulation where the parameters of the secondary dip are $\gamma_2 = -2.1\,{\rm km\,s^{-1}}$, $A_2 = 0.14$, $\sigma_2 = 8.0\,{\rm km\,s^{-1}}$ and $K_2 = 4.0\,{\rm km\,s^{-1}}$. The match is extremely good. In Fig. 10 we compare for the same simulation the slope of the relation BIS vs. $V_{\rm r}$ and the actual shape of the bisector for the maximum and minimum velocities observed and simulated.

We note that unfortunately the comparison of the bisector shapes (Fig. 10, right panels) have a bit of an uncertainty, given that we do not know the real shape of the bisector of the CCF of HD 41004 A. This seems to be particularly true for the bisector point nearest to continuum (see Fig. 7). We have thus introduced in Fig. 10 (lower right panel) a tentative error bar in this point, representative of the typical shift observed for the case of HD 13445 – Fig. 7. If in one hand this particular point is not used to compute the BIS, it will change the best general visual bisector shapes.

The important result at this point is that the plots clearly show that with the good set of parameters we can perfectly fit the observations. But to which extent can we constrain the results in order to characterize the properties of the CCF of HD 41004 B? In particular, it would be very interesting to obtain the values of σ_2 and K_2, that would permit us to derive the projected rotational velocity of HD 41004 B and the minimum mass for the companion orbiting it.

3.4. Quantifying the parameters

The results of the simulations described above have shown that there are some combinations of parameters for the secondary CCF that can match the observed amplitudes (in radial-velocity, BIS, $V_{\rm high}$ and $V_{\rm low}$), and the slope of the BIS vs. $V_{\rm r}$ relation. To constrain the models, we have first selected

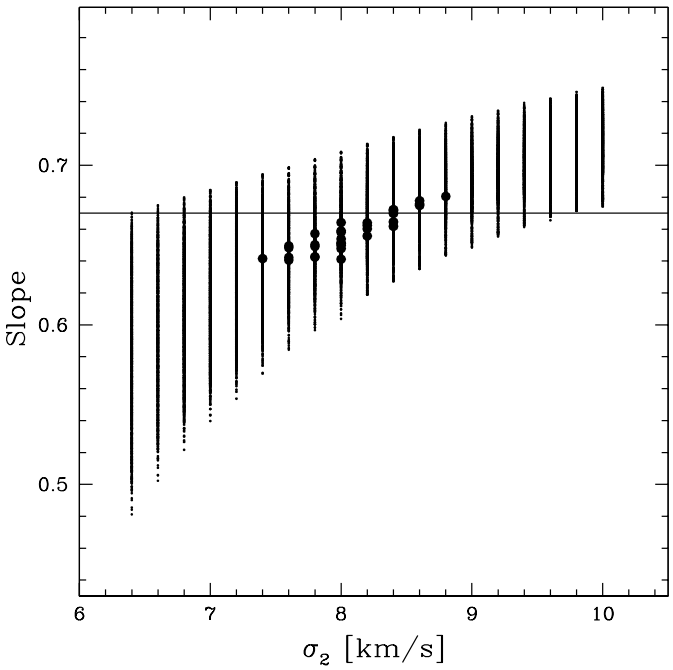

Fig. 11. Slope of the relation between BIS and V_r against σ_2 for all the simulations run. We can clearly see the trend of increasing slope with increasing σ_2. The larger dots represent only the simulations whose results are within the observational constraints (see text for further details). The line denotes the observed slope. We clearly see that σ_2 must have values close to 8 km s^{-1}.

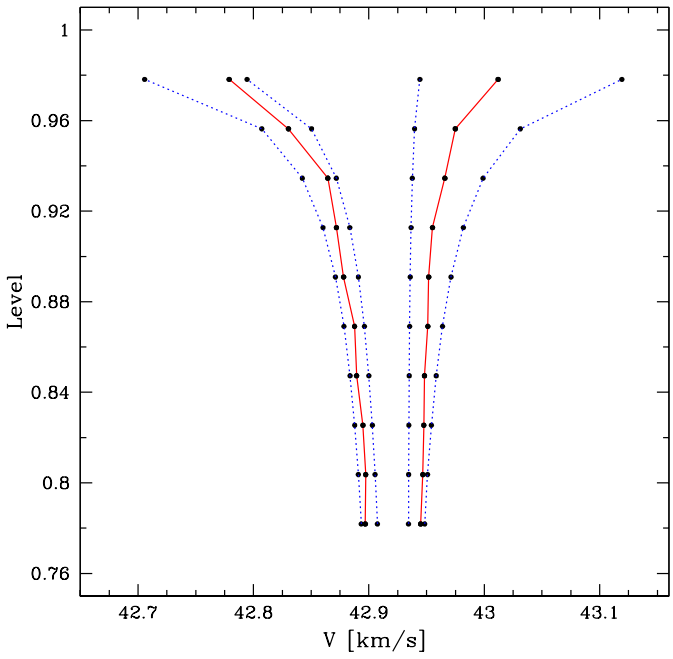

Fig. 12. Plot of the observed (solid lines) and the simulated (dotted lines) bisectors illustrating the effect of varying the amplitude K_2 in the simulations from 2.5 to 10 km s^{-1}. All the other parameters are as in Figs. 9 and 10.

all the simulations reproducing these quantities within 2-σ (corresponding to the uncertainty in the observed values, i.e. 4 m s^{-1} for the amplitudes and 0.06 for the slope).

We have then further compared the shape and "stretching" of the bisectors in order to better constraint the models. For this latter quantity, we have defined the difference in velocity between the upper bisector point (nearest to continuum, lets call it $V(A)$ and $V(A')$ in two bisectors corresponding to extreme velocity cases) and lower bisector point ($V(B)$ or $V(B')$) – see Fig. 10. The sum $|V(A) - V(B)| + |V(A') - V(B')|$, for example, is quite independent of the initial bisector shape, since it measures a differential displacement[13]. Based on Fig. 7 we have considered that we can estimate the observational values of $|V(A) - V(B)|$ and $|V(A') - V(B')|$ with a precision of 50 m s^{-1} (to take into account the bisector "C" shape), and that $|V(A) - V(B)| + |V(A') - V(B')|$ can be obtained with an uncertainty of 30 m s^{-1}, a value that seems reasonably conservative. But we note again that the absolute shape of the bisectors cannot be used as a comparison, since the real shape of the bisector for HD 41004 A is not known.

Although there is some degeneracy in the final results, some constraints can be set on the parameters of the secondary CCF. First, we have verified that the slope of the plot in Fig. 10 is most of all dependent on the width of the small dip. In all the simulations satisfying the criteria described above, σ_2 had values between 7.4 km s^{-1} and 8.6 km s^{-1}. This result, perfectly seen in Fig. 11, permits to determine σ_2 with a good precision: we estimate $\sigma_2 = 8 \pm 1$ km s^{-1}. Actually, we can interpret this dependence in light of the fact that the width of the smaller CCF will be the most important parameter controlling the extent to which a change in relative position between the two functions will induce a change in the measured radial-velocity (by fitting a Gaussian function to the final CCF) and in the BIS = $V_{\rm high} - V_{\rm low}$.

The knowledge of the width of the CCF of HD 41004 B means that we can estimate the projected rotational velocity of this star. Considering that the CCF of a non-rotating M dwarf with solar-metallicity is ~5 km s^{-1} (Delfosse et al. 1998a)[14], using the calibration presented in the Appendix we obtain a value of ~12 km s^{-1} for the $v \sin i$ of HD 41004 B. As we will see below, this value will permit to set constraints on the mass of the companion to this star (responsible for the 1.3-day period observed in radial-velocity).

For the other parameters (K_2, A_2, and γ_2), the constraints are not so strong. For example, there seems to be a clear relation that permits to have good models increasing A_2 and decreasing K_2. It would be very interesting, however, to derive K_2, since its value could give us an estimate for the mass of the companion orbiting HD 41004 B[15]. First, we have verified that it cannot have a very high value, or else we would find a flattening in one (or both) extremes of the radial-velocity curve (as already a bit noticed in the minimum of the the simulated velocities in Fig. 9), since the smaller CCF would be getting out of the

[13] This is true since the bisector is probably not strongly "C" shaped for a star of this spectral type.

[14] Such a value was obtained for the ELODIE spectrograph; with CORALIE, the value would be a bit smaller, but given the large obtained σ_2, the precise knowledge of this value is not crucial.

[15] In this sense γ_2 and A_2 are not particularly important to constraint.

bigger one. Furthermore, if K_2 were very high, the bisector shapes seen in Fig. 10 would be quite symmetrical (see Fig. 12). Based on the simulations satisfying all the criteria described above we can set an upper limit for K_2 around $5.2\,\mathrm{km\,s^{-1}}$ (all the *bona-fide* simulations gave K_2 between $2.8\,\mathrm{km\,s^{-1}}$ and $5.2\,\mathrm{km\,s^{-1}}$). From now on we will use the "worst case" value of $5.2\,\mathrm{km\,s^{-1}}$, i.e., the value that will correspond to the higher mass for the companion to HD 41004 B. As we will see below, this value will permit to estimate a tentative upper limit for the mass of the companion to HD 41004 B.

We could, in principle, try to see the variation in the observed CCF of HD 41004 AB due to the fact that it is constituted of the sum of two CCF's, one of which changes its position. To quantify the variation expected, we have subtracted two simulated "composed" CCF's corresponding to the extreme velocity cases of the position of the smaller one. For the parameters determined from our simulation, we can show that the difference is of the order of 0.3% (maximum). This small variation, within the observational errors of our measurements, is simply the result of the fact that the CCF of HD 41004 B is very large and shallow.

It is interesting to say that an analysis of the other parameters (width and depth) of the observed cross-correlation function of HD 41004 AB has revealed no special periodicity nor scatter. Such variations could be expected for a typical spectroscopic binary as a consequence of the variation of the relative position of the CCF's of the two stars. In agreement with the observations, our simulations show that these parameters do not change significantly. This is basically due to a combination of having $\sigma_2 \gg \sigma_1$ and $A_2 \ll A_1$.

4. A brown dwarf around HD 41004 B?

As shown in the previous section, the best way to explain the observed radial-velocity signal and CCF-bisector variations is to consider that HD 41004 B has a companion in a ∼1.3 day period orbit; considering a stellar mass of $0.4\,M_\odot$ (typical for a M2 dwarf), this value corresponds to a separation of only 0.017 AU[16]. Taking the maximum amplitude $K_2 < 5.2\,\mathrm{km\,s^{-1}}$ deduced from the simulations above, we can compute an upper limit for the minimum mass of the companion. The results give a value of $\sim 16\,M_{\mathrm{Jup}}$, strongly suggesting that the companion is in the typical brown-dwarf regime. We note, however, that according to our models, the mass could even be lower[17], and we cannot completely exclude that it is in the planetary regime. At this moment we prefer to remain cautious on this point, and we will thus consider this upper limit in the rest of the discussion; in this case, it is interesting to further discuss the implications of the discovery.

For these calculations we have considered a circular orbit. This is not only a direct result of the observed and simulated radial-velocity variations, but it is in fact expected for such a system. Actually, we can estimate the circularization timescale due to tidal dissipation in the companion's convective envelope (Rasio et al. 1996) – as done for HD 162020 by Udry et al. (2002). The value obtained is of the order of 10^8 yr, i.e., much shorter than the stellar age. In other words, we expect the system to be circularized[18].

The presence of a third body, in this case HD 41004 A, may induce eccentricity growth in the system composed of HD 41004 B+brown dwarf (Mazeh & Shaham 1979). If the period of this eccentricity modulation is shorter than the tidal circularization period, we could eventually expect that the semi-major axis of the short period system would decrease, simply because of the tidal dissipation occurring during the circularization of the orbit. To try to verify if the system could have survived to this effect, we have computed, using Eq. (3) in Mazeh & Shaham, the eccentricity modulation period expected for this system. The result gives a value around $1.5{\times}10^9$ yr. This is both longer than the circularization timescale and of the order of the derived stellar age, and thus we can expect that the system constituted of HD 41004 B+brown dwarf is stable. We further note that the timescale for orbital decay due to tidal dissipation in the stellar convective envelope is of the order of 10^{12} yr (Rasio et al. 1996).

We can also determine the stellar synchronization timescale for this system (HD 41004 B+brown dwarf). Using the equations in Udry et al. (2002)[19], we have obtained a value of 10^{7-8} yr. It is thus very likely that this system is synchronized. We can use this fact to estimate the "true" rotational velocity of HD 41004 B, since the synchronization implies that the rotational period of the star is the same as the orbital period of the companion (1.3 day). Taking a stellar radius typical for a M2 dwarf ($\sim 0.5\,R_\odot$), we obtain a value of $\sim 20\,\mathrm{km\,s^{-1}}$.

As we saw above, the width of the CCF of HD 41004 B can be fairly well constrained by our simulations, permitting to make a good estimate for the projected rotational velocity $v \sin i \sim 12.0\,\mathrm{km\,s^{-1}}$. This value implies a $\sin i \sim 0.6$. Within these conditions, we can deduce that the companion to HD 41004 B has a mass lower than $\sim 25\,M_{\mathrm{Jup}}$, placing it in the usually considered brown-dwarf regime.

At a separation of only ∼3.7 Solar radius, we can calculate that the Roche lobe of the companion is not filled. Using Eq. (2) in Eggleton (1983), we obtained a value of $R_{\mathrm{RL}} = 0.18\,a$, where a is the semi-major axis of the orbit. With $a = 3.7\,R_\odot$, we obtain $R_{\mathrm{RL}} \sim 0.7\,R_\odot$. This value is a factor of 7 larger than the typical radius of a $25\,M_{\mathrm{Jup}}$ brown dwarf[20]. No mass transfer is thus expected to occur.

[16] I.e., ∼7.5 stellar radius, considering that HD 41004 B has a radius of $0.5\,R_\odot$, typical for a M2 dwarf.

[17] Some models that fit the observations have K_2 as low as $2.8\,\mathrm{km\,s^{-1}}$, which would imply a value for the minimum mass of $\sim 8\,M_{\mathrm{Jup}}$.

[18] We note that the circularization timescale due to tidal dissipation in the stellar convective envelope (Zahn 1989) is much longer ($\sim 10^{10}$ yr).

[19] Taken from (Zahn 1989, 1992). For our case, we have considered the λ_2, t_{f}, and k^2 for a $0.6\,M_\odot$ star, the lower stellar mass tabled in Zahn (1994). Since the most important factor determining the synchronization rate is the ratio between the distance between the two objects and the radius of the star, and that these values do not change very steeply with stellar mass, we believe this is a good approximation.

[20] At an age of ∼1 Gyr, a brown dwarf with a mass around $0.03\,M_\odot$ has a radius around $0.1\,R_\odot$ – Chabrier et al. (2000).

5. Concluding remarks

We have presented the case of HD 41004 AB, a system composed of a K0V star and a 3.7 mag fainter M2 dwarf, separated by 0.5″. Radial-velocity measurements derived from CORALIE blended spectra of the two stars have unveiled a radial-velocity variation with a period of ~1.3 days and a small amplitude (~50 m s^{-1}), compatible with the expected signal due to the presence of a planetary companion to HD 41004 A. However, as we have seen, the combined radial-velocity, photometry and bisector analysis suggest that the best explanation for the observations is that the fainter HD 41004 B has a brown-dwarf companion. In this scenario, the observed low amplitude radial-velocity variation is due to the measure of a variation in the line profiles which is induced by the change of the relative position of the spectra corresponding to the two stellar components HD 41004 A and B.

If confirmed, the present discovery represents the first detection of a short-period brown-dwarf companion around a M2 dwarf. In particular, its estimated upper limit mass (~25 $M_{\rm Jup}$) puts it in the middle of the so-called brown-dwarf desert, a mass region (between ~20 and 40 $M_{\rm Jup}$) for which (almost) no short period companions to solar-type F, G, K (Halbwachs et al. 2000; Udry et al. 2001; Jorissen et al. 2001) and M (Marcy & Benitz 1989) dwarfs were found. The fact that HD 41004 B is a M dwarf makes us speculate that the formation of such systems is more likely for lower mass primaries, i.e. systems having mass ratios closer to unity (Duquennoy & Mayor 1991).

Armitage & Bonnell (2002) proposed a model to explain the existence of the brown-dwarf desert. One interesting feature of their model is that it predicts that no brown-dwarf desert should be observed for the companions around the lowest mass dwarfs; they set an upper limit of 0.1–0.2 $M_{\odot}$. Besides the fact that HD 41004 B is slightly more massive than this limit, the present case is interestingly similar to the predictions.

Recently, Zucker & Mazeh (2002) discussed an interesting correlation between the planetary mass and the orbital period. Their analysis strongly suggests that for single stellar systems, there is a lack of "high" mass planetary companions in short period orbits. On the other hand, Zucker & Mazeh have found that for stars in multiple systems, this correlation is no longer present. In particular, they have pointed out that in these latter cases, there seems to be a negative correlation between "planetary" mass and orbital period (see their Fig. 3). It is very interesting to see that the companion to HD 41004 B perfectly fits this trend.

A few works have tried to study the formation of planets (or low mass objects) around stars in multiple systems. Nelson (2000) showed that the formation of a planet in a disk is unlikely for equal mass binary systems with a separation lower than ~50 AU. On the other hand, Boss (1998) suggested that the influence of a companion might trigger "planetary" formation by disk instability. Although no strong conclusions are possible at this moment, the fact that HD 41004 B is in a double system with a separation that can be as low as ~20 AU is very interesting from the point of view of the formation of its companion.

Given the uncertainties in the shape of the observed bisector and in the models, we do not pretend to have a precise mass determination for the companion to HD 41004 B. Although we believe we have obtained a good estimate, one of the main goals of this paper was to illustrate the importance of combining the radial-velocity data with the bisector analysis. In other words, one important lesson to be taken from the presented results is that the bisector analysis was crucial to correctly interpret the observations.

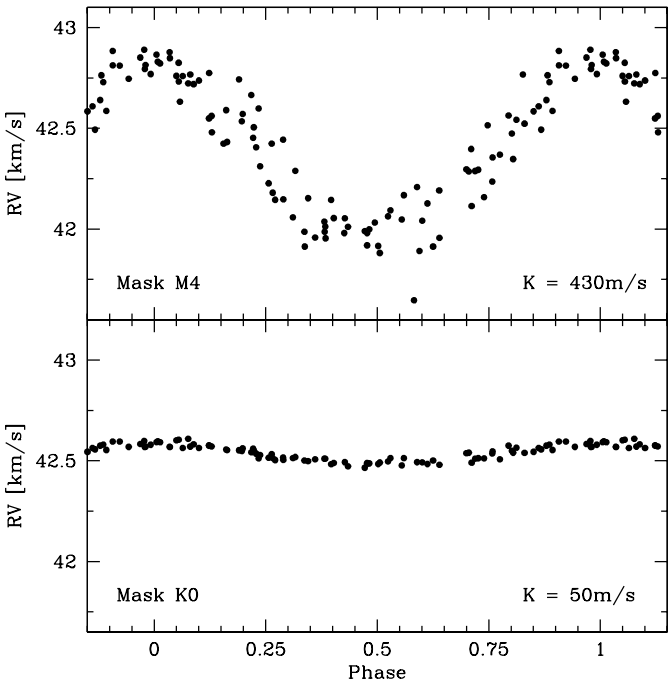

Fig. 13. Phase folded radial-velocity measurements of HD 41004 AB obtained using two different CCF masks. As expected, the amplitudes K obtained vary from mask to mask (see text). The vertical scales of the two plots is the same to facilitate a comparison.

It is important to caution that this kind of situation can also happen for long period systems. For those, the signal is very unlikely to have an intrinsic stellar activity origin, but we cannot exclude that it might originate from the presence of a "wobbling" stellar companion. It is very easy to find a situation where an undetected companion, a few tens of an arcsec distant, can be "contaminating" our analysis. Together with a good knowledge of the target star environment, in such a situation the bisector analysis seems to provide an unique tool to point out the exact origin of the radial-velocity variations.

In this sense we have analyzed (or re-analyzed) the bisectors for all the stars with planets discovered in the context of the CORALIE planet search programme[21]. We did not find any significant correlation between $V_{\rm r}$ and BIS. We can thus remain confident that the presence of a planetary companion is the best way of explaining the radial-velocity variations in these systems.

Besides the bisector analysis, one other way of testing a radial-velocity variation for such cases may involve the measurement of the radial-velocity using different sets of lines, or different spectral regions. If the radial-velocity variation is due to the presence of a planet, we can expect that every

[21] See obswww.unige.ch/~udry/planet/planet.html

spectral region/line will give us about the same velocity amplitude (but not necessarily the same γ-velocity). The fact that for HD 41004 AB the amplitude in radial velocity was different using the cross-correlation mask constructed specially for the bisector analysis (Queloz et al. 2001b) from the one obtained using the "classical" mask is very telling (see Sect. 2.3). In Fig. 13 we can further see two phase folded diagrams for the radial-velocities of HD 41004 AB obtained using two different CCF masks. As we can see, if we use a mask specially constructed for the radial-velocity determination of M4 dwarfs (Delfosse et al. 1998b), i.e. a spectral type close to the one of HD 41004 B, we obtain a much higher amplitude in radial-velocity than for the case of using a mask constructed for K0 dwarfs. This difference is expected since in such a case, the difference between the CCF's of HD 41004 A and HD 41004 B is much smaller (the M dwarf spectrum is enhanced relatively to the K dwarf), being thus the influence of the "small" CCF stronger. A similar situation (although not as strong) is seen when comparing the amplitudes obtained using the K0 and the F0 masks.

This kind of analysis can, in principle, serve as a test, if the study of the bisector is not possible. But we note that for radial-velocity variations induced by the presence of dark spots in the stellar photosphere, i.e. where the same phenomenon is affecting all spectral lines in about the same way, we do not expect a strong difference between the radial-velocity amplitudes obtained using different spectral lines.

Finally, it is interesting to say a few words about other possible ways of confirming the current detection. Given the short period of the brown dwarf around HD 41004 B, the probability that we are able to observe a transit is quite high. In a first approximation, the magnitude variation expected in such a transit is around 10^{-3} (for the A+B system), a value that does not seem too low. But a simpler way of confirming this case would pass by doing high-resolution spectroscopy (and velocity measurements) of HD 41004 B. However, this is not an easy task, since the two components of HD 41004 AB are separated by only 0.5″. Unfortunately, there are no available high-resolution spectrographs attached to an Adaptative Optics system in the southern hemisphere capable of accomplishing this task. The use of the Hubble Space Telescope (HST) might represent a solution. Else, the solution may pass by using high-resolution near-IR spectroscopy, since at those wavelengths the flux of HD 41004 B is much closer to the one from HD 41004 A.

Appendix A: Determination of v sin i and [Fe/H] from the Cross-Correlation Function

One interesting property of the Cross-Correlation Function (CCF) is that any stellar "phenomenon" capable of influencing the lines included in the correlation mask (e.g. the line profiles) will be reflected on the CCF itself (i.e. on its shape, depth and width). In other words, the CCF represents an "average" spectral line amidst those used in the correlation mask (Mayor 1985). The profile and intensity of the CCF is thus a convolution between the profile due to the intrinsic stellar atmospheric parameters affecting the lines in the mask (like the global

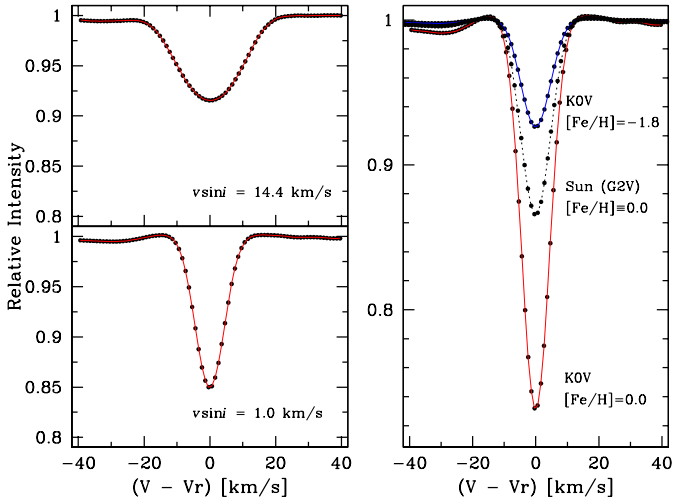

Fig. A.1. *Left panels*: plot of the CORALIE CCF for two stars with different projected rotational velocities. This figure illustrates the effect of the v sin i on the CCF; *right panel*: plot illustrating the variation of the surface of the CCF due to changes in the metallicity and temperature.

abundance, thermal broadening, pressure broadening, or microturbulence), and the macroscopic macroturbulence and rotational velocity of the star (Gray 1992), without forgetting the instrumental profile, characteristic of a given instrument. In the case of CORALIE, given that the correlation mask is constructed using mostly weak neutral lines in the spectrum of a standard star (a K0 dwarf), the properties of the resulting CCF are basically dependent on the physical quantities controlling the properties of a "typical" neutral weak metal line. For a detailed description of the Cross-Correlation technique we refer to Baranne et al. (1996) and Pepe et al. (2002).

From a practical point of view, this give us the possibility to obtain stellar quantities that are reflected on the spectral lines directly by analyzing the parameters of the CCF. We can even hope to build specific masks for different kinds of lines, each sensitive to a different stellar parameter. Let us see in the next sections how this can be used to derive two important quantities from the CORALIE CCF: the v sin i and the stellar metallicity[22].

A.1. A calibration of the projected rotational velocity v sin i

The Gaussian width of a weak spectral line of a "non-rotator" depends basically on the spectral type and luminosity class. This is mostly related to the fact that temperature and surface gravity are the main variables controlling both the line strength and broadening, due to the temperature and pressure effects[23].

[22] For more details, and a broader discussion about the errors for the two calibrations presented below, we refer to Santos (2002).

[23] Two other variables, the abundance and the magnetic field, will be discussed below. Note also that we will "forget" about natural broadening, since it is constant for each line. Furthermore, we consider that the limb-darkening properties are the same for a given temperature and surface gravity.

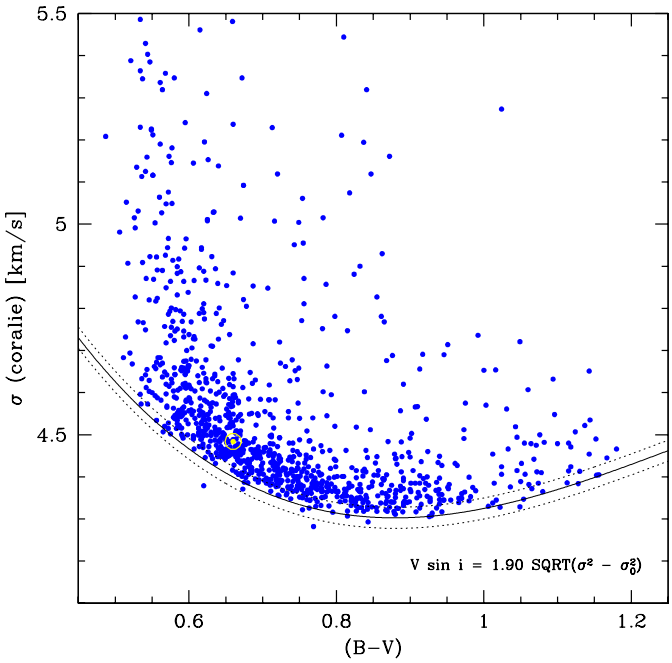

Fig. A.2. Plot of the Gaussian width of the CORALIE CCF (expressed in km s^{-1}) vs. $B-V$. The lower envelope (solid line) determines the locus of the stars with zero rotational velocity. The two dashed lines represent the uncertainty of 0.025 km s^{-1} in the position of the lower envelope of the points.

These variables actually indirectly control other broadening parameters like the macro- and micro-turbulence (Gray 1992). At the end, the only broadening parameter left that is definitely independent of the intrinsic stellar atmosphere properties is the projected rotational velocity ($v \sin i$).

Actually, considering that the instrumental profile is constant for each star and does not change in time for a given spectral type and luminosity class (which is a reasonable thing to do for such stable instruments like CORALIE) we can expect that every star will have approximately the same "zero" CCF width – hereafter called σ_0 – and for a constant temperature and surface gravity, the "excess" width that the lines (i.e. the CCF) might present is then mostly due to the effect of the rotational velocity.

There are, however, two other physical quantities that can (in principle) change significantly the value of σ_0: the metallicity and the magnetic field. In fact, the higher the metal content of a star, the higher the number of saturated lines; this saturation will cause a slight increase in σ_0. In our case this effect is not very strong, since the cross-correlation masks are based mainly on weak lines. As for the magnetic field, it is known that changing its intensity will change the Zeeman spliting of the spectral lines, thus broadening their profiles. This fact can even be used to obtain an estimation of the stellar magnetic field (e.g. Borra et al. 1984; Queloz et al. 1996). However, it has been shown by Benz & Mayor (1984) that the line broadening due to the effect of the magnetic field is only important for late K and M stars. Since this effect would be quite complicated to take into account, and it is probably not important for most of the stars in the CORALIE survey, we will not consider it in the rest of this discussion.

Benz & Mayor (1984) have successfully shown that the width of the CORAVEL CCF is well correlated with the $v \sin i$ of a star. These two variables can be related by:

$$v \sin i = A \sqrt{\sigma^2 - \sigma_0^2} \quad \text{(A.1)}$$

where σ represents the measured Gaussian width of the CCF, σ_0 the value of the expected σ for a "non-rotator" of a given spectral type and luminosity, and A is a constant relating the "σ-excess" to the actual projected rotational velocity of the star ($v \sin i$). We are, of course, considering that the CCF of a rotating star can be approximated by a Gaussian. As shown by Queloz et al. (1998) this is true up to velocities of ~20 km s^{-1}, the regime we are mostly interested in.

Using the same idea, we have used the CORALIE CCF to calibrate a relation between the σ obtained with this instrument and the $v \sin i$ for solar type dwarfs. There are basically two things to do. The first is the determination of σ_0. This quantity can be obtained simply by adjusting the lower envelope of the distribution of points in a plot of σ vs. $B-V$ (this latter quantity is quite well related with temperature)[24]. In this envelope we will, in principle, find the non-rotator stars. We note that most of the stars observed with CORALIE are dwarfs, and there are probably no objects with luminosity classes lower than IV. Such a plot is seen in Fig. A.2, and the adjusted lower envelope is well described by:

$$\sigma_0 = 6.603 - 6.357\,(B-V) + 5.533\,(B-V)^2 - 1.454\,(B-V)^3. \quad \text{(A.2)}$$

It is interesting to say a few words about Eq. (A.2). As can be seen from Fig. A.2, the fitted function decreases up to values of $B-V \sim 0.9$ (where it has a minimum) and then increases again towards higher $B-V$ values. In the low $B-V$ regime, this decrease might simply be explained by a decrease in the macroturbulent dispersion (Gray 1992). On the other side, for high $B-V$ values, the increase in σ_0 is probably due to the increase in the damping constant due to van der Waals broadening, that can be shown to increase with decreasing temperature. Furthermore, up to a spectral type of K5, neutral metallic lines increase in strength, thus increasing the number of saturated lines (for a constant abundance). As discussed in Benz & Mayor (1984), the increase of the magnetic field as a funcion of increasing spectral type might also be responsible for the increase in σ_0 after a given spectral type. Together with these physical processes, variations resulting from the way the CCF mask is optimized (Baranne et al. 1979; Benz & Mayor 1984) might also introduce some trend[25]. It is, however, difficult to quantify exactly what is the net effect of all these processes.

It is important to mention that after all the metallicity does not seem to play an important role in the determination

[24] Since the $B-V$ is a widespread index available for all the stars in the CORALIE sample, it is a particularly suitable variable to use.

[25] We expect σ to be slightly different in the red and in the blue part of the spectrum since the "lines" in the mask are in average slightly larger in the red; consequently, this might introduce a small increase of the CCF with increasing spectral type.

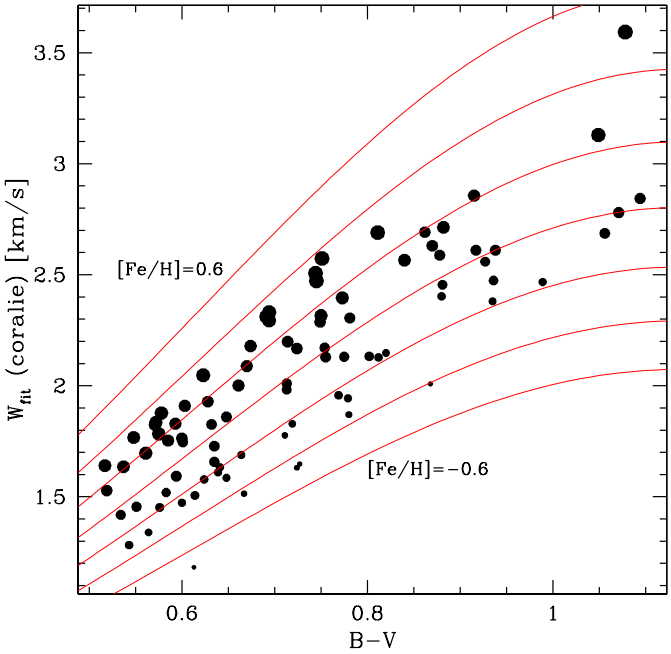

Fig. A.3. Plot of the CORALIE CCF surface $W_{\rm fit}$ as a function of $B-V$. $W_{\rm fit}$, expressed in km s^{-1}, is defined as $\sqrt{2\,\pi}\cdot\sigma_{\rm fit}\cdot A_{\rm fit}$, where $\sigma_{\rm fit}$ and $A_{\rm fit}$ are the Gaussian width (in km s^{-1}) and depth of the measured CCF, respectively. The lines represent regions with [Fe/H] = constant. The size of the points is proportional to the spectroscopically determined metallicity. The spectroscopic metallicities were taken from Santos et al. (2001a,b).

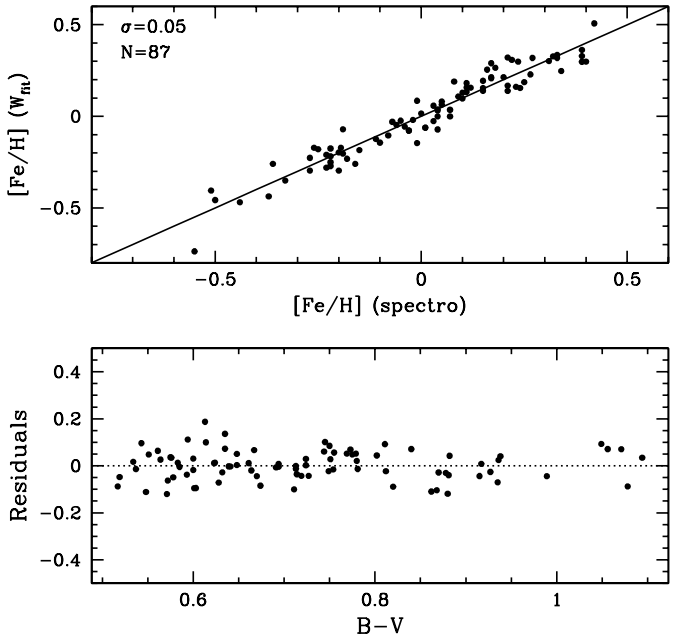

Fig. A.4. *Upper panel*: comparison between the spectroscopic and calibrated [Fe/H]. *Lower panel*: residuals of the calibration as a function of $B-V$; no dependence is found. The spectroscopic metallicities were taken from Santos et al. (2001a,b).

of σ_0. A few tests were done, separating the stars in Fig. A.2 into different metallicity bins. The result showed that the effect is very small, and difficult to quantify amidst the noise in the lower envelope of the points. The interpretation of this is, as mentioned above, probably quite simple: since we are dealing with weak lines in the linear part of the curve of growth, the saturation effect is not expected to be very strong.

The other variable in Eq. (A.1) we need to determine is A, i.e., the constant relating the $v \sin i$ to the "excess" width of the CCF. This can be done in the same way as in Queloz et al. (1998): by measuring the variation of σ as we convolve the CCF of non-rotating stars with a given rotational profile (Gray 1992). For CORALIE we find $A = 1.9 \pm 0.1$, close to the value obtained for ELODIE (Queloz et al. 1998). In any case, the final value of $v \sin i$ is not strongly dependent on errors in A.

The technique described above represents a very simple way of obtaining precise projected rotational velocities for dwarfs, simply as a by-product of the precise radial-velocity measurements. In particular, the calibration permits us to obtain quite easily values for the $v \sin i$ for all the stars in the CORALIE planet search programme.

A.2. A calibration of the metallicity

Another variable that can easily be obtained from the CCF of a star is its metallicity. This has been firstly done by Mayor (1980) for the CORAVEL CCF, a calibration that was later improved by Pont (1997).

As mentioned above, the mask used for CORALIE is mainly built out of a set of weak neutral spectral lines (from a template K0 spectra). Since most of them are iron lines (the main contributor for the line opacity in solar type stars), we can expect that the surface (i.e. the Equivalent Width) of the CCF is well related to the [Fe/H] of a star.

Furthermore, the fact that we are dealing with weak neutral lines in solar-type stars implies that the surface of the CCF will be basically independent on the microturbulence and the surface gravity. These would have an important effect if we were not dealing with lines that are in the linear part of the curve of growth, since the broadening produced by these effects would act to de-saturate the lines, increasing thus their equivalent widths. Furthermore, it can be shown that weak lines of an element for which most of it is in the next ionization state (most of the iron in a solar-type star is in the form of Fe II) are quite insensitive to pressure changes. The surface of the CCF will thus mainly depend on the temperature (well correlated with $B-V$) and abundance (see Fig. A.1).

To calibrate a relation between the surface of the CORALIE CCF (hereafter $W_{\rm fit}$) and the iron abundance expressed by [Fe/H], we have used a set of stars for which we had obtained precise [Fe/H] values using a detailed spectroscopic analysis (Santos et al. 2001a,b). The fit, shown in Fig. A.3 gives:

$$\begin{aligned}[\mathrm{Fe/H}] \;=\; & 2.573 + 4.587\,\log W_{\rm fit} \\ & -8.142\,(B-V) + 3.583\,(B-V)^2\end{aligned} \qquad \text{(A.3)}$$

a calibration valid for $0.52 < B-V < 1.1$, $1.18 < W_{\rm fit} < 3.59$ and $-0.55 <$ [Fe/H] < 0.42. As expected, the figure shows that for a given metallicity, the equivalent width of the spectral lines (i.e. the surface of the CCF) increases with decreasing temperature. This is the "normal" behaviour of a weak metallic

line in this temperature regime (up to spectral types around K5, $B - V \sim 1.2$).

A comparison between the metallicities obtained from the CCF surface and a spectroscopic analysis shows that the fit has a remarkable small dispersion (0.05 dex – Fig. A.4), similar to the uncertainties in the spectroscopic determinations. Furthermore, there seems to be no special systematics with temperature. We can thus trust on this calibration to obtain precise values of [Fe/H] for the stars in the CORALIE planet search programme without any long and arduous spectroscopic analysis. We note that the metallicities obtained this way are spectroscopic determinations, since we are using spectral line information. Although we cannot exclude that for a particular star the result might not be as precise as a detailed spectroscopic analysis determination, at least in statistical studies this is certainly an extremely accurate technique.

Acknowledgements. We want to thank T. Mazeh for the interesting discussions and suggestion, and S. Bouley and R. Leguet for having kindly observed HD 41004 AB at the SAT on two nights each, as well as the anonymous referee whose comments helped a lot to improve the clarity of the paper. We wish to thank the Swiss National Science Foundation (Swiss NSF) for the continuous support for this project. The photometry was obtained as part of an extensive study of GK type eclipsing binaries supported by the Danish Natural Science Research Council. Support from Fundação para a Ciência e Tecnologia, Portugal, to N.C.S. in the form of a scholarship is gratefully acknowledged. This research has made use of the Simbad database, operated at CDS, Strasbourg, France.

References

Allende Prieto, C., García López, R., Lambert, D. L., & Gustafsson, B., ApJ, 527, 879
Alonso, A., Arribas, S., & Martínez-Roger, C. 1996, A&A, 313, 873
Armitage, P. J., & Bonnell, I. A. 2002, MNRAS, 330, L11
Baranne, A., Queloz, D., Mayor, M., et al. 1996, A&AS, 119, 373
Baranne, A., Mayor, M., & Poncet, J. L. 1979, Vistas Astron., 23, 279
Benz, W., & Mayor, M. 1984, A&A, 138, 183
Borra, E. F., Edwards, G., & Mayor, M. 1984, ApJ, 284, 211
Boss, A. 1998, BAAS, 30, 1057
Butler, R. P., Tinney, C. G., Marcy, G. W., et al. 2001, ApJ, 555, 504
Chabrier, G., Baraffe, I., Allard, F., & Hauschildt, P. 2000, ApJ, 542, 464
Delfosse, X., Forveille, T., Perrier, C., & Mayor, M. 1998a, A&A, 331, 581
Delfosse, X., Forveille, T., Mayor, M., et al. 1998b, A&A, 338, L67
Donahue, R. A. 1993, Ph.D. Thesis, New Mexico State University
Duquennoy, A., & Mayor, M. 1991, A&A, 248, 485
Eggleton, P. P. 1983, ApJ, 268, 368
ESA 1997, The HIPPARCOS and TYCHO catalogue, ESA-SP 1200
Flower, P. J. 1996, ApJ, 469, 355
Gray, D. 1992, in The observation and analysis of stellar photospheres (Cambridge Univ. Press)
Halbwachs, J. L., Arenou, F., Mayor, M., Udry, S., & Queloz, D. 2000, A&A, 355, 581
Henry, T. J., Soderblom, D. R., Donahue, R. A., & Baliunas, S. L. 1996, AJ, 111, 439
Jones, B. F., Fischer, D., & Soderblom, D. R. 1999, AJ, 117, 330
Jorissen, A., Mayor, M., & Udry, S. 2001, A&A, 379, 992
Kurucz, R. L. 1993, CD-ROMs, ATLAS9 Stellar Atmospheres Programs and 2 km s^{-1} Grid (Cambridge: Smithsonian Astrophys. Obs.)
Lucy, L. B., & Sweeney, M. A. 1971, AJ, 76, 544
Marcy, G. W., & Benitz, K. J. 1989, ApJ, 344, 441
Mayor, M. 1985, in Stellar Radial Velocities, IAU Colloq., 88, 21
Mayor, M. 1980, A&A, 87, L1
Mazeh, T., & Shaham, J. 1979, A&A, 77, 145
Nelson, A. F. 2000, ApJ, 537, L65
Noyes, R. W., Hartmann, L. W., Baliunas, S. L., et al. 1984, ApJ, 279, 763
Olsen, E. H. 1994a, A&AS, 106, 257
Olsen, E. H. 1994b, A&AS, 104, 429
Olsen, E. H. 1993, A&AS, 102, 89
Olsen, E. H. 1984, A&AS, 57, 443
Pepe, F., Mayor, M., Galland, F., et al. 2002, A&A, in press
Pepe, F. A., Mayor, M., Benz, W., et al. 2000a, in VLT Opening Symposium From extra-solar planets to brown-dwarfs, ESO Astrophys. Symp. Ser., ed. J. Bergeron, & A. Renzini (Springer-Verlag, Heidelberg), in press
Pepe, F., Mayor, M., Queloz, D., & Udry, S. 2000b, in Planetary Systems in the Universe: Observation, Formation and Evolution, IAU Symp. 202, ed. A. Penny, P. Artymowicz, A.-M. Lagrange, & S. Russel, ASP Conf. Ser., in press
Pont, F. 1997, Ph.D. Thesis, Geneva University
Queloz, D., Mayor, M., et al. 2001a, The Messenger, 115, 1
Queloz, D., Henry, G. W., Sivan, J.P., et al. 2001b, A&A, in press
Queloz, D., Allain, S., Mermilliod, J.-C., Bouvier, J., & Mayor, M. 1998, A&A, 335, 183
Queloz, D., Babel, J., & Mayor, M. 1996, in 9th workshop on Cool stars, stellar systems, and the Sun, ed. R. Pallavicini, & A. K. Dupree, APS Conf. Ser., 109, 627
Rasio, F. A., Tout, C. A., Lubow, S. H., & Livio, M. 1996, ApJ, 470, 1187
Saar, S. H., Butler, R. P., & Marcy, G. W. 1998, ApJ, 498, L153
Saar, S. H., & Donahue, R. A. 1997, ApJ, 485, 319
Santos, N. C. 2002, Ph.D. Thesis, Univ. of Geneva (available at `http://obswww.unige.ch/~santos`)
Santos, N. C., Israelian, G., & Mayor, M. 2001a, A&A, 373, 1019
Santos, N. C., Israelian, G., & Mayor, M. 2001b, in proceedings of the 12th workshop on Cool Stars, Stellar Systems, and the Sun
Santos, N. C., Mayor, M., Naef, D., et al. 2000, A&A, 361, 265
Schaller, G., Schaerer, D., Meynet, G., & Maeder, A. 1992, A&AS, 96, 269
Schuster, W. J, & Nissen, P. E. 1989, A&A, 221, 65
Sneden, C. 1973, Ph.D. Thesis, University of Texas
Udry, S., Mayor, M., Naef, D., et al. 2002, A&A, in press
Udry, S., & Mayor, M. 2001, in First European Workshop on Exo/Astrobiology, Frascati, May 2001, ESA SP, in press (`obswww.unige.ch/Preprints/Preprints/udry_frascati.ps.gz`)
Udry, S., Mayor, M., Naef, D., et al. 2000a, A&A, 356, 590
Zahn, J.-P. 1994, A&A, 288, 829
Zahn, J.-P. 1992, in Binaries as Tracers of Stellar Formation, Bettmeralp, Switzerland, ed. A. Duquennoy, & M. Mayor (Cambridge Univ. Press), 253
Zahn, J.-P., & Bouchet, L. 1989, A&A, 223, 112
Zucker, S., & Mazeh, T. 2002, ApJ, 568, L113